

# Supporting Information for Coupled 2D quantum dot films for next generation solar cells: electronic structure and anomalous light absorption behaviour

R. V. H. Hahn,<sup>†</sup> M. Califano,<sup>‡</sup> S. Rodríguez-Bolívar,<sup>†</sup> and F. M. Gómez-Campos<sup>\*,†</sup>

<sup>†</sup>*Departamento de Electrónica y Tecnología de Computadores, Facultad de Ciencias,  
Universidad de Granada, 18071, Granada, Spain*

<sup>‡</sup>*Pollard Institute, School of Electronic and Electrical Engineering, University of Leeds, LS2  
9JT, UK*

E-mail: fmgomez@ugr.es

## Simple model

Within the tight-binding approximation for a 1D crystal using a single state with  $s$ -symmetry as the basis, the band can be approximated as:

$$E_{q_x} \approx E_0 - 2 \cos(q_x d) \times \int \phi(x)V(x)\phi(x-d)dx \quad (1)$$

$E_0$  being the band mean energy,  $\phi(x)$  the wave function of the isolated CQD state creating the band,  $V(x)$  the CQD potential,  $\phi(x-d)$  the eigenstate wave function centred at the neighbouring CQD located at a distance  $d$ . In the tight-binding picture we can expand this result to an orthorhombic 3D array with different values of the lattice constants along each

direction as follows:

$$E_{\vec{q}} \approx E_0 - 2 \sum_{j=x,y,z} \cos(q_j |\vec{R}_{j,1}|) \times \int \phi(\vec{r}) V(\vec{r}) \phi(\vec{r} - \vec{R}_{j,1}) d\vec{r} \quad (2)$$

where  $\vec{R}_{j,1}$  stands for the CQD nearest-neighbour positions along the  $x$ ,  $y$  and  $z$  directions that, *a priori*, may have different lengths.

Several results can be derived from this model. Firstly, an estimate of the total miniband width,  $W_{band}$ , for 3D CQD arrays with arbitrary lattice constants along each direction can be extracted from the above integrals as:

$$W_{band} \approx \sum_{j=x,y,z} 4 \int \phi(\vec{r}) V(\vec{r}) \phi(\vec{r} - \vec{R}_{j,1}) d\vec{r} \quad (3)$$

To clarify this point, Fig. 5 (main text) shows the values of  $4 \int \phi(\vec{r}) V(\vec{r}) \phi(\vec{r} - \vec{R}_{z,1}) d\vec{r}$  for several interdot distances, starting from the closest 1D packing (one-bond length surface-to-surface separation) in each material. The IB width for a 3D array made of these CQDs can be obtained from Fig. 5 (main text) by summation of the miniband widths, considering the interdot distance along each direction.

A first validation of this toy model can be obtained from the results shown in Fig. 3 (main text), where the IB widths in panels (a,e,i) and (d,h,l), relative to a single 2D layer and a 3D array, respectively, approximately correspond to twice and three times the miniband width per dimension for the shortest interdot distance in Fig. 5 (main text).

Furthermore, this model can also be used to obtain an estimate for the IB widths in stacked layers with arbitrary inter-layer distances. In this case we need to consider that, under the tight-binding approximation, the eigenenergies of a finite system can be related to the ones of an infinite system by a particular sampling of the reciprocal lattice vectors (specifically,  $q = \frac{i\pi}{(n+1)d}$ , where  $i = 1, \dots, n^1$ , and  $d$  is the interdot distance). In particular, the eigenenergies of a 1D finite array with  $n$  CQDs can be related to the band energies of the infinite system

as:

$$E_{q_x} \approx E_0 - 2 \int \phi(x)V(x)\phi(x-d)dx \times \cos\left(\frac{i\pi}{n+1}\right). \quad (4)$$

In a single (infinite) 2D layer, the system is periodic in the in-plane directions and, therefore, the miniband widths can be estimated as twice the width per dimension shown in Fig. 5 (main text), relative to the specific inter-dot separation of the layer. The stacking of  $n$  layers introduces an additional term to this width

$$W_{stack} \approx 2 \int \phi(\vec{r})V(\vec{r})\phi(\vec{r}-\vec{R}_{z,1})d\vec{r} \times \left[ \cos\left(\frac{\pi}{n+1}\right) - \cos\left(\frac{n\pi}{n+1}\right) \right] \quad (5)$$

due to the finiteness of the system along the stacking direction, which leads to a splitting of the minibands related to the sampling of the reciprocal lattice vectors mentioned above (the arguments of the cosines in Eq. (8) (main text) are precisely the extrema of the  $q$  sampling interval, i.e., the  $q$ -values relative to  $i = 1$  and  $i = n$ ).

## Effective transitions considered in the simplified absorption calculations

We have analysed the photon absorption in stacks of 2D layers of InP, InAs and InSb CQDs as indicated in the main text. The minibands of the CQD single layer were labelled with numbers corresponding to their energy values at the  $\Gamma$  point, starting from 0 for the lowest energy miniband. Firstly, photon absorption transitions in a CQD single layer were grouped into three different photon energy sets, corresponding with energy intervals where the three absorbance peaks (or group of peaks) were observed. The groups correspond to the three different transitions (from the lowest to the highest energies): i) from the intermediate to the conduction miniband(s), ii) from the valence to the intermediate miniband(s) and iii) from the valence to the conduction minibands. Exceptionally, in InP there are transitions from valence to the conduction minibands with photon energies close to the ones from the valence

to the intermediate miniband. These transitions have been assigned to the latter group because their absorbance peaks correspond to energies in the same absorbance peaks than transitions from the valence to the intermediate miniband. In a second step, the maximum of each peak (or group of peaks) was identified, and the photon absorbance between minibands with values over 10 % of that maximum were indicated in the following tables.

Finally, we represented in Fig. 6, Fig. 7 and Fig. 8 in the main text the photon absorbance

<b>InP single layer</b>											
<b>IB to CB transitions</b>				<b>Mainly VB to IB transitions</b>				<b>VB to CB transitions</b>			
<b>Pol 100</b>		<b>Pol 010</b>		<b>Pol 100</b>		<b>Pol 010</b>		<b>Pol 100</b>		<b>Pol 010</b>	
<b>Initial</b>	<b>Final</b>	<b>Initial</b>	<b>Final</b>	<b>Initial</b>	<b>Final</b>	<b>Initial</b>	<b>Final</b>	<b>Initial</b>	<b>Final</b>	<b>Initial</b>	<b>Final</b>
9	10	9	10	0	9	0	9	0	11	0	10
	11		11	1	9	1	9		12		12
	12		12	3	9				13		13
				6	12			1	12	1	12
				8	10				13		13
								3	10		
									11		

Figure 1: Transitions within a single InP 2D layer with  $\alpha > 10\% \alpha_{\max}$  (see main text for details). The minibands of the CQD single layer are labelled as  $j = 0, \dots, j_{tot}$ , starting from the lowest energy miniband at the  $\Gamma$  point. Valence minibands are from 0 to 8, the intermediate band is 9, and the conduction minibands are from 10 to 15.

curves using only those transitions and compared to the curves using all the transitions in a single layer. For a N-layer system, the number of minibands is N times larger than for the single layer. We assumed a correspondence between the minibands of the N-layer system and the single layer: we sorted in groups of N minibands the N-layer system minibands, and identified the group with one miniband of the single layer, following the same order. For example, the first N minibands in the N-layer system were assigned to the single layer miniband labelled as 0, the next N minibands were assigned to the single layer miniband labelled as 1... We used this criterion for the representation of photon absorption of 5-layer and 10-layer stacks in the above referred to figures, compared to the photon absorption

InAs single layer											
IB to CB transitions				VB to IB transitions				VB to CB transitions			
Pol 100		Pol 010		Pol 100		Pol 010		Pol 100		Pol 010	
Initial	Final	Initial	Final	Initial	Final	Initial	Final	Initial	Final	Initial	Final
7	8	7	8	1	7	0	7	2	8	2	8
	9		9	3	7	3	7		9		9
	10		10	4	7	4	7		10	5	8
								5	8		9
									10		10
								6	8	6	9
									9		10
									10		

Figure 2: Transitions within a single InP 2D layer with  $\alpha > 10\% \alpha_{\max}$  (see main text for details). The minibands of the CQD single layer are labelled as  $j = 0, \dots, j_{\text{tot}}$ , starting from the lowest energy miniband at the  $\Gamma$  point. Valence minibands are from 0 to 6, the intermediate band is 7, and the conduction minibands are from 8 to 14.

InSb single layer											
IB to CB transitions				VB to IB transitions				VB to CB transitions			
Pol 100		Pol 010		Pol 100		Pol 010		Pol 100		Pol 010	
Initial	Final	Initial	Final	Initial	Final	Initial	Final	Initial	Final	Initial	Final
6	8 – 16	6	8 – 16	2	6	2	6	2	7 – 10	2	9
				3	6	3	6		12 – 16		12 – 16
				4	6	4	6	3	7 – 10	3	7
						5	6		12 – 16		10
								4	7 – 16		12 – 14
								5	7		16
									9 – 16	4	8 – 10
											12 – 15
										5	8
											9
											11 – 13

Figure 3: Transitions within a single InSb 2D layer with  $\alpha > 10\% \alpha_{\max}$  (see main text for details). The minibands of the CQD single layer are labelled as  $j = 0, \dots, j_{\text{tot}}$ , starting from the lowest energy miniband at the  $\Gamma$  point. Valence minibands are from 0 to 5, the intermediate band is 6, and the conduction minibands are from 7 to 16.

considering all the bands.

In the tables of Fig. 1, Fig. 2 and Fig. 3 of this Supplementary Information we show the transitions we found relevant for a single layer in each energy interval.

## Modelling of Dirac delta in the photon absorption calculations

The Dirac delta in Fermi's Golden Rule, accounting for the energy conservation in the photon absorption process, has been modelled in this work as a normalized window function as follows:

$$\delta(E_f - E_i - \hbar\omega) \approx \begin{cases} 0 & \text{if } |E_f - E_i - \hbar\omega| > \Delta/2 \\ \frac{1}{\Delta} & \text{if } |E_f - E_i - \hbar\omega| \leq \Delta/2 \end{cases} \quad (6)$$

$E_f$  being the electron final energy,  $E_i$  the electron initial energy,  $\hbar\omega$  the photon energy and  $\Delta E$  the uncertainty in the energy conservation due to the Dirac delta modelling. The photon energy is, therefore, obtained as the difference between the final and initial electron state energies. For every sampling in the reciprocal space, almost every photon absorption yields a different photon energy (for example, due to symmetry considerations in the reciprocal space, the exact photon energy could be repeated in films a maximum of four times along the calculations). This results in a very noisy and unphysical light absorption profile.

In order to solve these issues, we analysed adequate values for  $\Delta E$ . We concluded that, for the samplings of the reciprocal space used in this work, dividing the whole range of photon energies in 250 intervals is an adequate compromise between the physical details and the noisy profile.

We considered the transitions between two particular minibands in a QD film using several window function widths. In order to obtain a general result, we modelled two minibands in a square 2D array film as:

$$E_0(q_x, q_y) = \epsilon_0 - \frac{W_0}{4} [\cos(q_x a) + \cos(q_y a)] \quad (7)$$

$$E_1(q_x, q_y) = \epsilon_1 + \frac{W_1}{4} [\cos(q_x a) + \cos(q_y a)] \quad (8)$$

$\epsilon_0$  and  $\epsilon_1$  are the miniband central energies,  $W_0$  and  $W_1$  are the respective miniband widths,  $a$  is the lattice constant and  $E_1 > E_0, \forall q_x, q_y$ . The absorbed photon energy for an electron in the lowest miniband and state  $(q_x, q_y)$  is obtained as  $E_{ph}(q_x, q_y) = E_1(q_x, q_y) - E_0(q_x, q_y)$ . In consequence, the photon energy ranges from  $\epsilon_1 - \epsilon_0 - \frac{W_1+W_0}{2}$  to  $\epsilon_1 - \epsilon_0 + \frac{W_1+W_0}{2}$ . For generalisation purposes, we can normalize this energy range from 0 to 1 corresponding to the minimum and maximum photon energy respectively.

In Figure 4 we show the absorption peak when the energy range is divided into 150, 75, 50, 25 and 15 intervals. It is noticeable from the figure that sampling the absorption peak in the order of a few tens of intervals (25 and 15 particularly) provides a smooth absorption curve.

In our study, the individual peaks corresponding to miniband-to-miniband transitions of

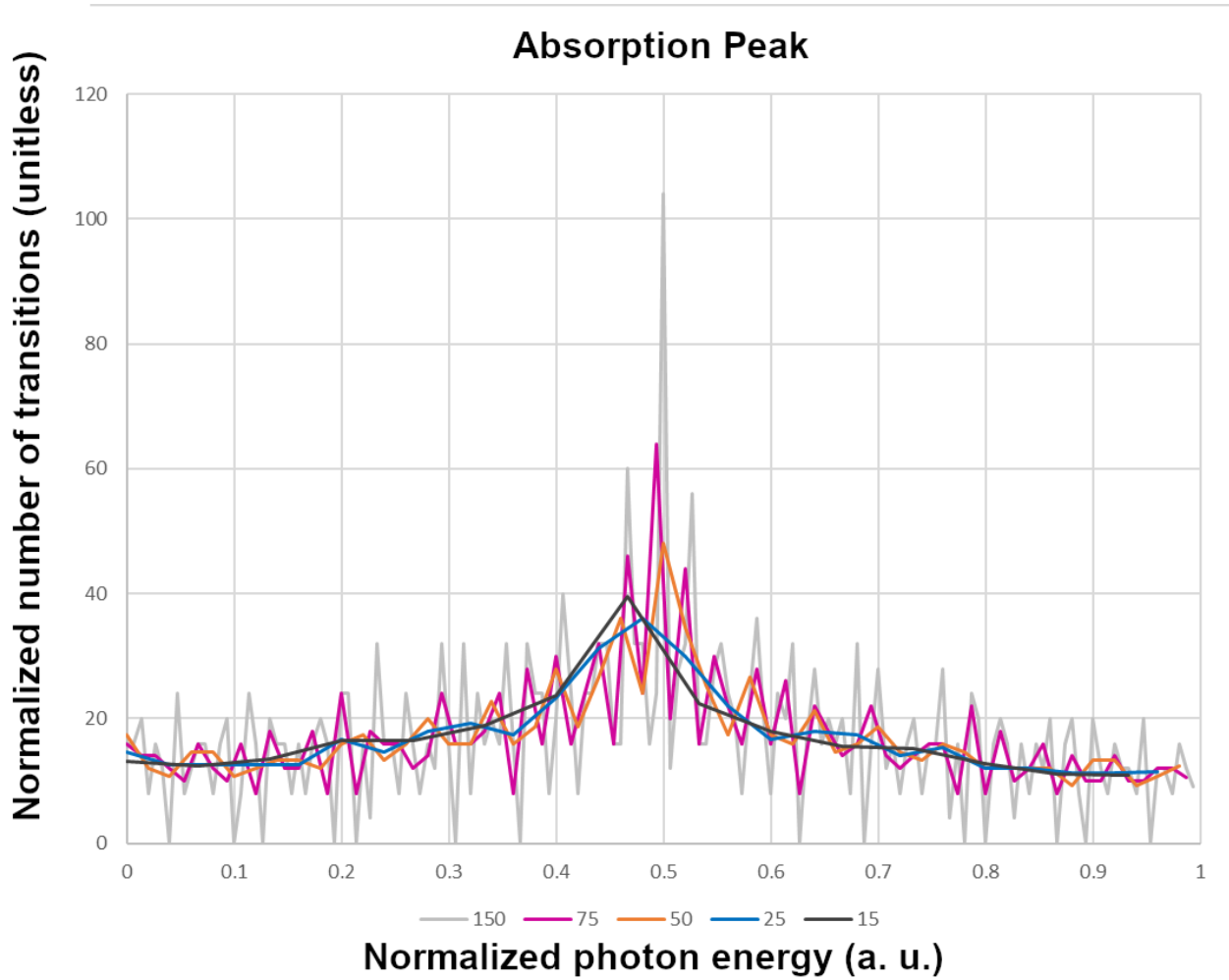


Figure 4: Different samplings of the absorption peak between two minibands using a normalized energy range (0, the smallest energy difference between minibands; 1, the greatest energy difference between minibands). The figure shows the absorption coefficient computed using 150, 75, 50, 25 and 15 intervals to sample the whole range.

the absorption profile are in the order of several tens of meV, similarly to the Figure 4, a smooth photon absorption profile can be obtained if the peaks are sampled in a few tens of intervals, i. e. intervals of around 1-10 meV width. That is the reason why a photon range of 2.5-3 eV is adequately sampled using 250 intervals, and from that the Dirac delta is adequately modelled with a window function.

## References

1. Skibinsky Gitlin, E. S. Estudio del transporte y absorción de luz en redes periódicas de puntos cuánticos de semiconductor. 2021; <http://hdl.handle.net/10481/68189>.